Lecture 19

"Unusual" and Superluminous Supernovae

For the observer, an unusual supernova is one that is atypically faint or bright, long or short, or has an unusual time history or spectral characteristics (e.g. repeats has more than one optical peak or has very broad or narrow lines).

For the theorist, they are events that cannot be explained using (just) the traditional core-collapse or thermonuclear central engines (i.e., neutrino transport and white dwarf detonation. They require, for example:

- Circumstellar Interaction
- Magnetar energy input
- Pair instability
- Black hole accretion

Circumstellar interaction

Consider stationary matter with local density ρ impacted an expanding spherical shell moving with speed v_s. The swept-up matter is forced to move at speed v_s, but the overall velocity of the piston, which has large, but finite mass slows with time. A reverse shock propagates into the expanding material. The momentum flux at the interface is

$$\rho v_s^2 \text{ dyne cm}^{-2}$$

The rate at which this does work (per cm^2) is $\rho v_s^2 \frac{dr_s}{dt}$ or

$$\rho v_s^3 \text{ dyne cm}^{-2}\left(\frac{\text{cm}}{\text{sec}}\right) = \rho v_s^3 \text{ erg cm}^{-2}\text{ s}^{-1}$$

Multiplying by the area of the shell

$$L_{CSM} = 4\pi r_s^2 \rho v_s^3 \text{ erg s}^{-1}$$

Actually, considering conservation of momentum 1/2 the energy goes to acelerating the matter and is not radiated

$$L_{CSM} = 2\pi r_s^2 \rho v_s^3 = \frac{\dot{M}}{2}\frac{v_s^3}{v_{wind}}$$

E.g. A star has a pre-explosive mass loss rate of 5 x 10^{-5} M_O yr^{-1}. The star is a red supergiant so its wind speed is slow – 50 km s^{-1} It explodes producing a shock whose outer edge moves at 10,000 km s^{-1}. The initial luminosity from CSM interaction is

$$L = \frac{\dot{M}}{2}\frac{v_s^3}{v_{wind}} = \frac{5\times10^{-5}}{2}\frac{2\times10^{33}}{3.16\times10^{7}}\frac{\left(10^9\right)^3}{5\times10^{6}}$$
$$= 3\times10^{41} \text{ erg s}^{-1}$$

This is bright enough to add a substantial contribution to a supernova luminosity. For a higher mass loss rate, greater shock speed, or slower wind speed the supernova light curve could be dominated by the interaction. The mass loss may have been in the final years of the star's life. What matters is the density inside 10^{16} cm (1000 AU). CSI plays a major role in Type IIn supernovae. Sometimes LBV's are associated with SLSN and the episodic mass loss may be very high.

Multicomponent lines in spectra. ~100 km/s and ~1000's km/s.

Evolves with time. Multiple shocks?

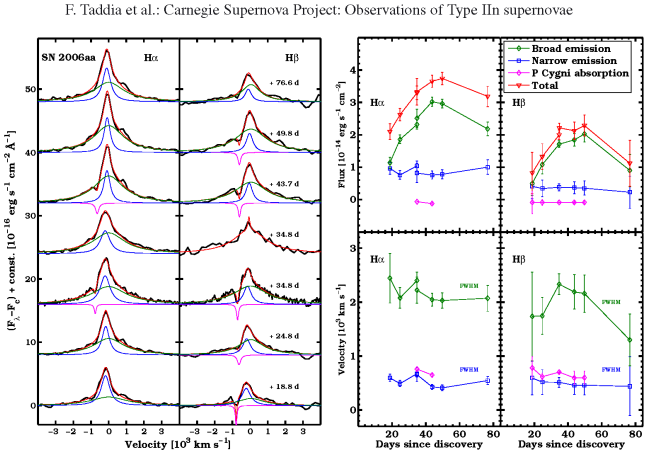

SN IIn – characterized by narrow spectral lines of hydrogen. May be bright x-ray or radio sources. Typically brighter than SN IIp. May become strong IR sources. Grain formation? Wide variety of light curve shapes and luminosities. Mean M_B = -18.7. ~ 10% of core-collapse supernovae

SN IIn

Inferred mass loss 10^{-4} to 0.01 M_O y^{-1}
Taddia et al (2013)

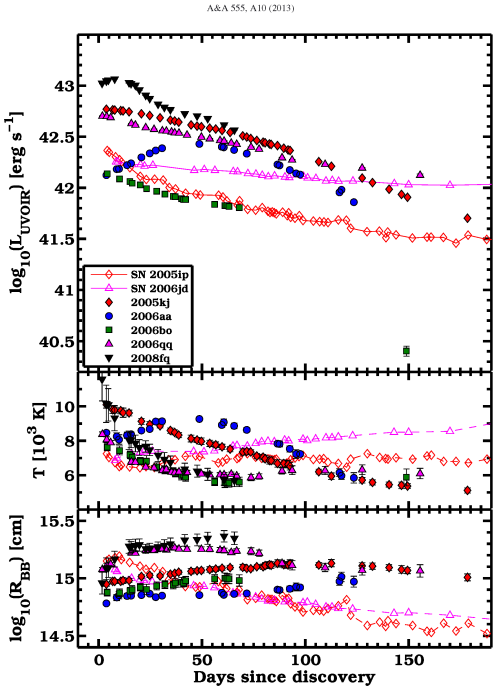

Superluminous Supernovae (SLSN) – M < -21 Gal-Yam (2012)

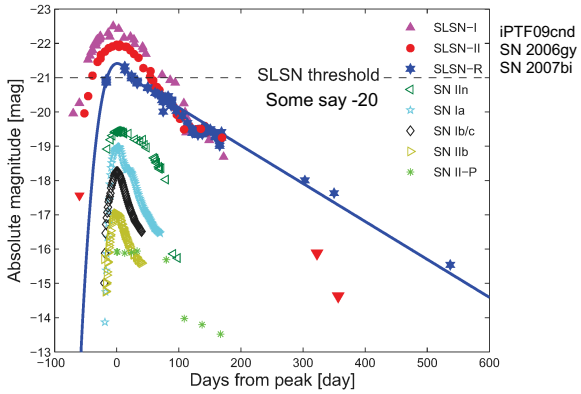

Fig. 1.— The luminosity evolution (light curve) of supernovae. Common SN explosions reach peak luminosities of $\sim 10^{43}\,\mathrm{erg\,s^{-1}}$ (absolute magnitude > -19.5). The new class of super-luminous SN (SLSN) reach luminosities ~ 10 times higher. The prototypical events of the three SLSN classes (SLSN-I PTF09cnd, Quimby et al. 2011; SLSN-II SN 2006gy, Smith et al. 2007, Ofek et al. 2007, Agnoletto et al. 2009; and SN 2007bi, Gal-Yam et al. 2009) are compared with a normal Type Ia SN (Nugent template), Type IIn SN 2005cl (Kiewe et al. 2011), the average Type Ib/c light curve from Drout et al. (2012), the Type IIb SN 2011dh (Arcavi et al. 2011) and the prototypical Type II-P SN 1999em (Leonard et al. 2002). All data are in the observed R band. See SOM for additional details.

SN 1999em was unusually faint for a SN IIp

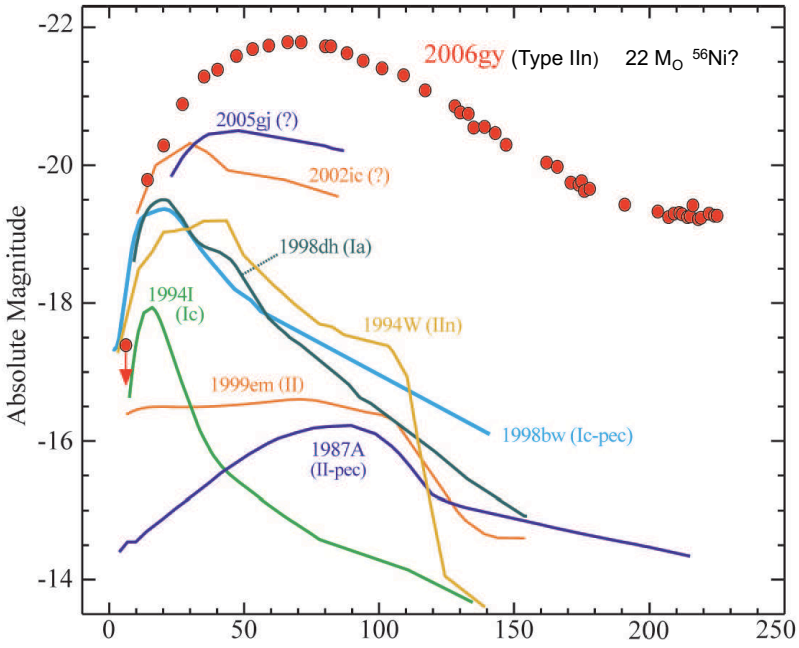

Smith et al (2010)

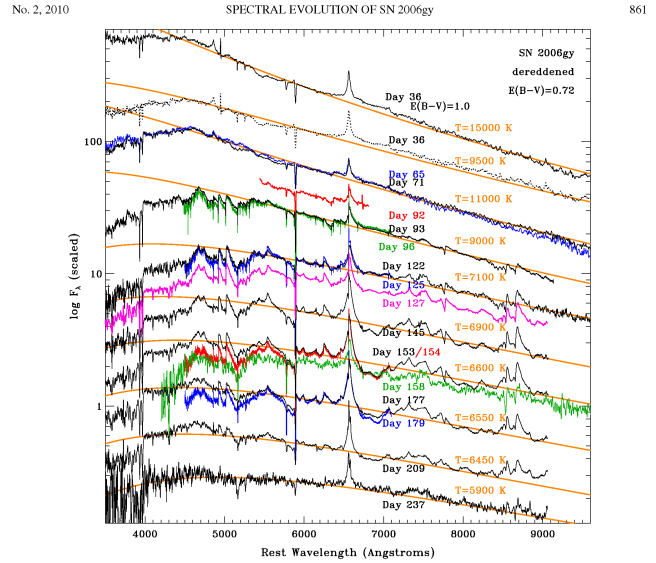

Several SLSN – II. Typically this class displays narrow lines suggestive of CSM interaction. Diverse light curves. Inferred mass loss ~ .0001 - .01 M_O yr^{-1} Chatzopoulos et al (2011)

The Astrophysical Journal, 729:143 (20pp), 2011 March 10

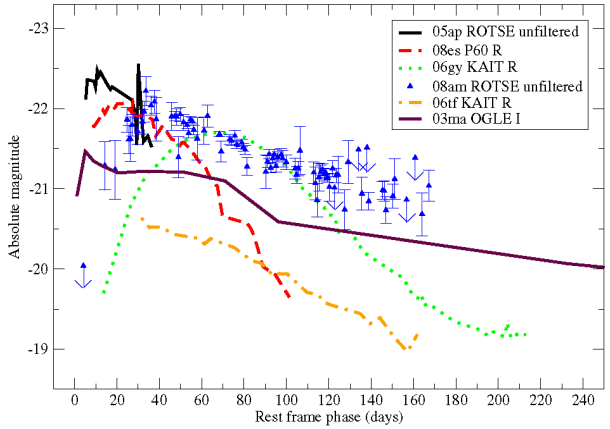

Figure 13. Comparison of the rest-frame light curve of SN 2008am with those of other luminous supernovae: SN 2003ma (Rest et al. 2009), SN 2005ap (Quimby et al. 2007a), SN 2006gy (Smith et al. 2007), SN 2006tf (Smith et al. 2008), and SN 2008es (Gezari et al. 2009).

For Type I SLSN (Gal-Yam 2018)

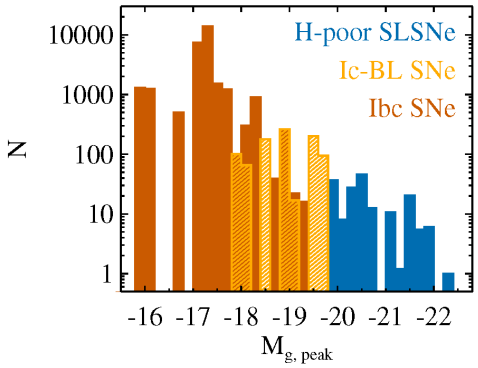

Figure 1

A histogram of the luminosity of SLSNe-I, SNe Ic and SNe-Ic-BL from PTF with a volumetric correction accounting for the detectability of more luminous events out to larger distances, adapted with permission from De Cia et al. (2018). The more luminous events (blue) also share spectral similarity according to Quimby et al. (2018) suggestion a threshold of $M_g = -19.8$ mag may separate SLSNe-I from lower-luminosity events.

SLSN-I

Nicholl et al (2015)

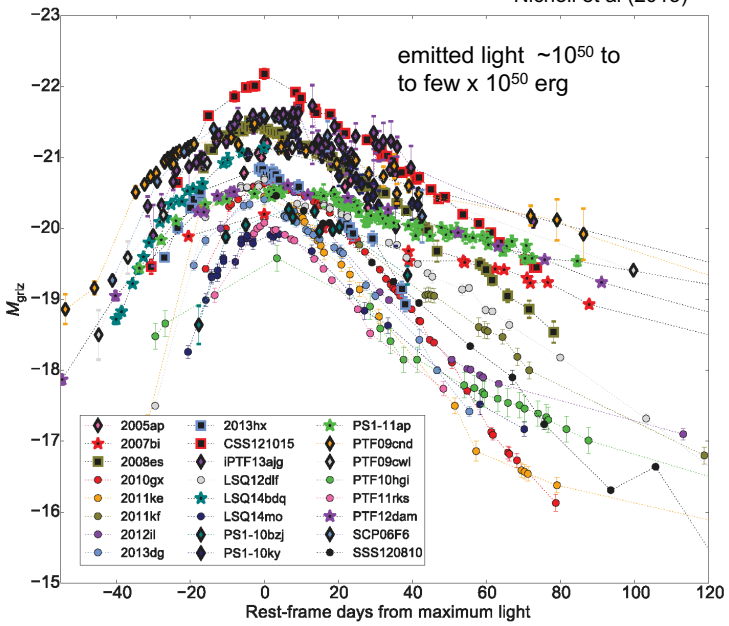

Some have rapid rise times:

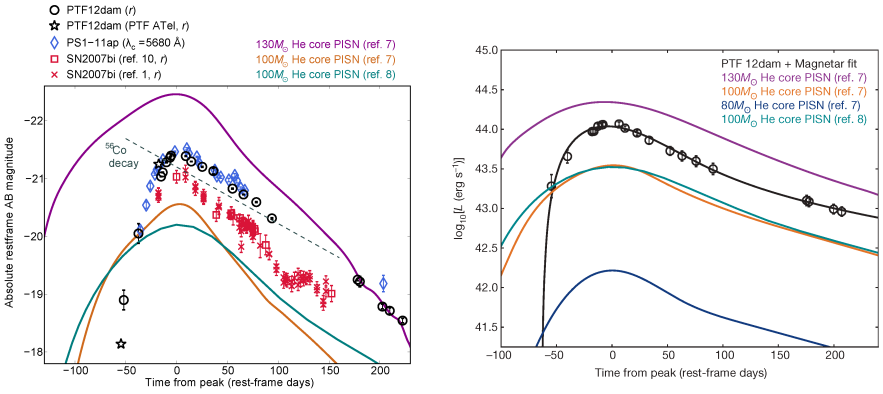

Nicholl et al (2013) – slowly fading rapidly rising events NOT pair instability supernovae

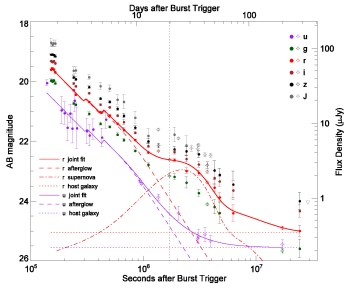

Optical afterglow of very long GRB 111209A at z = 0.677. GRB lasted more than 10,000 s

Blue points are the light curve of SN 2011 kl associated with the GRB. Other curves are for SLSN (green and red points) or Type Ic-BL associated with previous GRBs and XRFs.

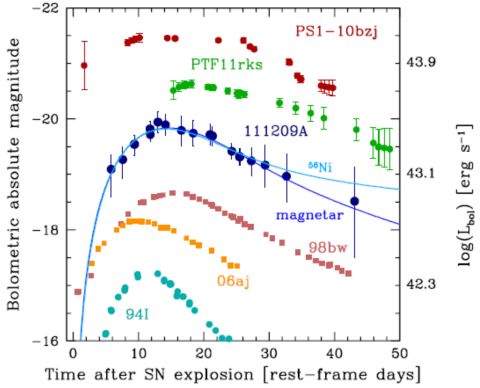

Magnetars:

(Woosley 2010); Kasen and Bildsten (2010)

- 10% or more of neutron stars are born as “magnetars”, neutron stars with exceptionally high magnetic field strength (B ~ $10^{14\text{-}15}$ gauss) and possibly large rotation rates.
- A rotational period of 6 ms corresponds to a kinetic energy of 5 x 10^{50} erg. A high rotational rate may be required to make a magnetar. Where did this energy go?
- High field strengths give a very significant contribution to the explosion energy, but weaker fields actually make brighter supernovae (for a given rotational energy). This reflects the competition between adiabatic energy loss and diffusion.

The initial explosion might not be rotationally powered but assume a highly magnetized pulsar is nevertheless created. Using the same dipole formula as for pulsars (WH10, but goes all the way back to Gunn and Ostriker in 1971)

$$E_{51}(t=0) = 0.2\left(\frac{10\ \text{ms}}{P_0}\right)^2$$

$$E_{51}(t) = \left(\frac{B_{15}^2\, t}{4\times 10^4} + \frac{1}{E_{51}(t=0)}\right)^{-1} \qquad t_{peak} = \frac{6Ic^3}{B^2R^6\Omega_i^2} = 1.3\,B_{14}^{-2}P_{10}^2\ \text{yr} \quad \text{(BK10)}$$

$$L = 10^{49}\ B_{15}^2\left(\frac{E_{51}(t)}{20.}\right)^2 \propto B_{15}^{-2}\ t^{-2} \ \text{ at late times}$$

Using the two parameters B_{15} and P_0 a great variety of curves that go up (as the energy diffuses out through the expanding supernova – see formula by Inserra et al 2013) and then down (as the magnetar spins down) can be fit. B~ few x 10^{14} G will contribute significantly to the light curve. But validity of simple dipole formula?

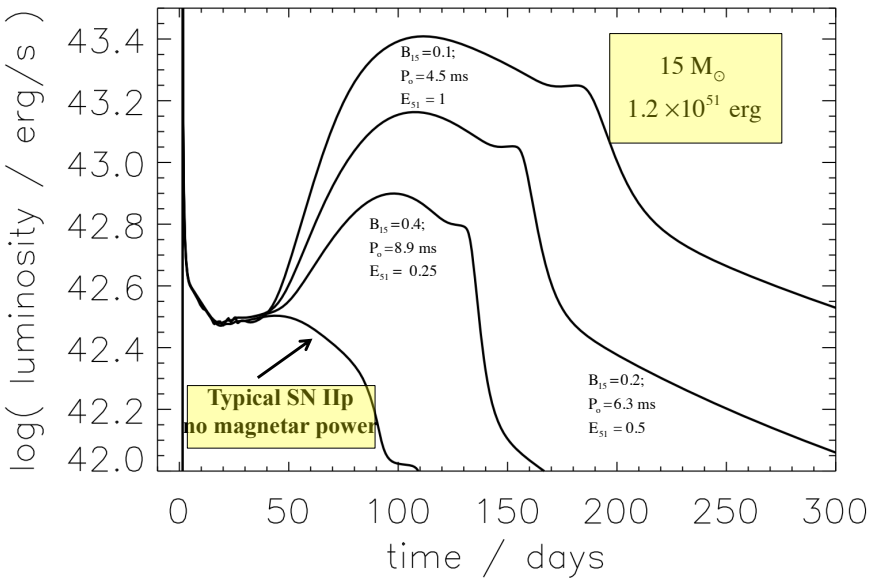

Maeda et al 2007; Woosley 2010;
Kasen and Bildsten 2010

Observed Type Ic Supernovae vs Magnetar Models

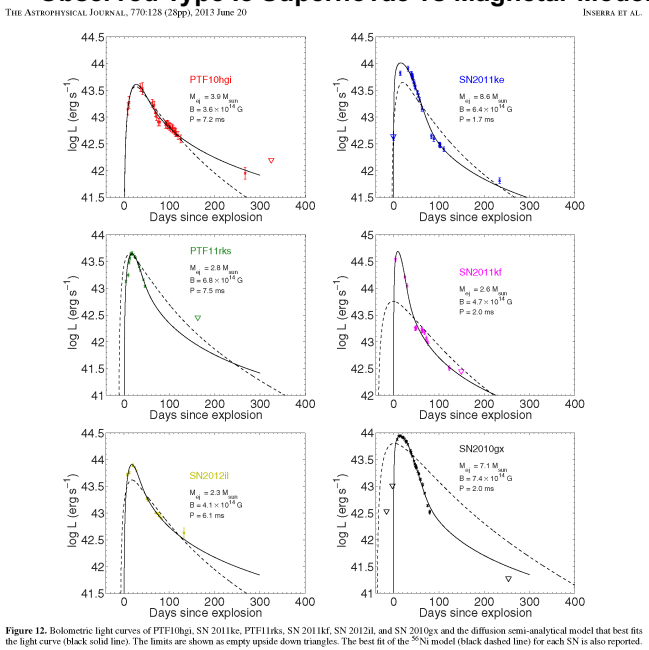

Figure 12. Bolometric light curves of PTF10hgi, SN 2011ke, PTF11rks, SN 2011kf, SN 2012il, and SN 2010gx and the diffusion semi-analytical model that best fits the light curve (black solid line). The limits are shown as empty upside down triangles. The best fit of the ^{56}Ni model (black dashed line) for each SN is also reported.

Complicated by multi-dimensional effects

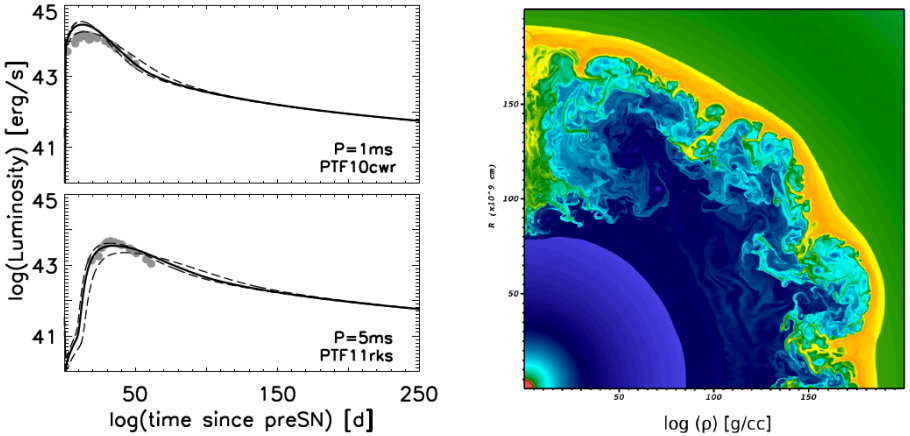

Chen, Woosley and Sukhbold (2015)

Black Hole Accretion -

Radially symmetric accretion into a non-rotating black hole is not expected to provide any energy, but if the accreting material has sufficient angular momentum to form a disk, a very large power is in principle possible.

There are two ways an accreting black hole can power an outflow. 1) through dissipation in the disk – generally referred to as the Blandford-Payne (BP) mechanism and 2) if the black hole rotates rapidly, by extracting angular momentum from the hole – generally referred to as the Blandford-Znajek (BZ) mechanism.

Approximate formulae can be derived for each, essentially by dimensional analysis. There are much more rigorous derivations and many numerical experiments. See recent papers by McKinney (2005, 2006, 2012) and Tchekhovskoy (2008, 2011)

Blandford-Payne –disk luminosity

$L \sim Area \times energy\ density \times speed$

$Area \sim \pi R_s^2 \quad with\ R_S = \frac{2GM}{c^2} \qquad v_A \approx c$

$Energy\ density \sim \frac{B^2}{8\pi}$

$$L_{BP} \sim few \times 10^{50}\ B_{15}^2 \left(M / M_\odot\right)^2 \text{ erg s}^{-1}$$

Aside:
If the field reaches equipartition strengths

$$\frac{B^2}{8\pi} \sim \rho v_{orbit}^2 \sim \rho v_{freefall}^2$$

Area * energy density * v

$$\sim \pi r^2 \rho v_{freefall}^3 \sim \dot{M} v_{freefall}^2$$

And if v ~ c

L ~ constant $\dot{M}c^2$ constant << 1

Blandford-Znajek – spin luminosity

For constant Ω $\frac{dE}{dt} = \frac{\Omega}{2}\frac{dL}{dt}$ where L is the total angular momentum L = I Ω and I $\approx$2/5 MR^2. The angular momentum changes due to the torque

$$\frac{dL}{dt} \sim \frac{B_r B_\varphi}{4\pi} R^3$$

$$B_{\varphi \max} \sim \frac{\Omega R}{c} B_r$$

$$\text{Power} = \frac{dE}{dt} \sim \frac{\Omega}{2}\frac{\Omega R B_r^2}{4\pi c} R^3 \sim \frac{\Omega^2 B_r^2 R^4}{8\pi c}$$

Due to many uncertainties in the derivation this is usually treated as an upper bound. The Swartzschild radius is substituted for R and the overall expression multiplied by an uncertain factor of 0.01 to 0.1.

$$L_{BZ} = 0.01 \text{ to } 0.1\ \frac{\Omega^2 B_r^2 R_s^4}{c} \approx 0.01 \text{ to } .1\ B_r^2 a^2 R_s^2 c$$

where a is the Kerr parameter $\approx \frac{\Omega R_s}{c} < 1$

$$L_{BZ} \sim 10^{50} B_{15}^2 \left(\frac{M}{M_\odot}\right)^2 a^2 \text{ erg s}^{-1}$$ for fudge factor 0.03

nb. what to use for the Schwarzshild radius for a ~1 complicates things a bit

Results are often parameterized by some uncertain efficiency factor (which depends on the black hole rotation rate and field in the accreting matter) times the accretion rate.

McKinney (2005) gives a maximum efficiency of 0.148 $\dot{M}c^2$ of which 0.068 $\dot{M}c^2$ is in a jet, but for Kerr parameters < 1 the efficiency falls off rapidly.

Accretion could be due to a failed explosion and the and the formation of a collapsar (Woosley 1993; MacFadyen and Woosley 1999) or fallback (MacFadyen et al 2001; Dexter and Kasen 2013). Even 1% efficiency and a low accretion rate gives a lot of power – if there is sufficient angular momentum to form a disk. An accretion rate of 10^{-7} M_O s^{-1} would give a power of 1.8 x 10^{45} erg s^{-1}, far greater than any observed supernova. I M_O y^{-1} would give 5 x 10^{44} erg s^{-1}
Quite possibly the outflow would be beamed.

The big problem is having enough angular momentum to make a disk

BH accretion is one of the two leading explanations for GRBs

BH accretion may also produce very long transients by when the outer layers of the star fall in (Woosley and Heger 2012; Quataert and Kasen 2012) that could be confused with tidal disruption.

If a disk can form black hole accretion from fall back could power SLSNe (Dexter and Kasen 2013)

The Astrophysical Journal, 772:30 (12pp), 2013 July 20

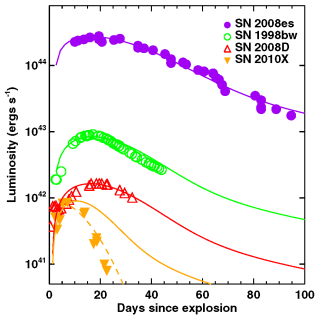

L ~ $t^{-5/3}$ at late times

Potentially huge energy reservoir

Starved for angular momentum

Uncertain physics

Pair Instability

Barkat, Rakavy and Sack (1967)
Rakavy, Shaviv and Zinamon (1967)

A purely thermonuclear mechanism. Simple physics compared with the rest. The equation of state shows that for temperatures around 1 – 3 x 10^9 K (3kT = 260 – 770 keV ~ $m_e c^2$) a large number of electron-positron pairs begins to exist in thermal equilibrium with the gas. Creating the mass of these pairs takes energy that does not contribute to pressure, so, for awhile, an increase in temperature does not contribute as much to the pressure as it would have if the pair masses had not needed to be created. As a result a contraction does not raise the temperature and pressure enough to balance the stronger gravity in the denser state. The structural adiabatic index Γ goes slightly below 4/3 and the star becomes unstable.

As the star begins to collapse though it has unburned fuels, chiefly oxygen but also carbon, neon, and silicon, that it burns rapidly. If the contraction has not gone too far (encountered the photo-disintegration instability) and if enough fuel remains, the burning turns the implosion around and causes an explosion.

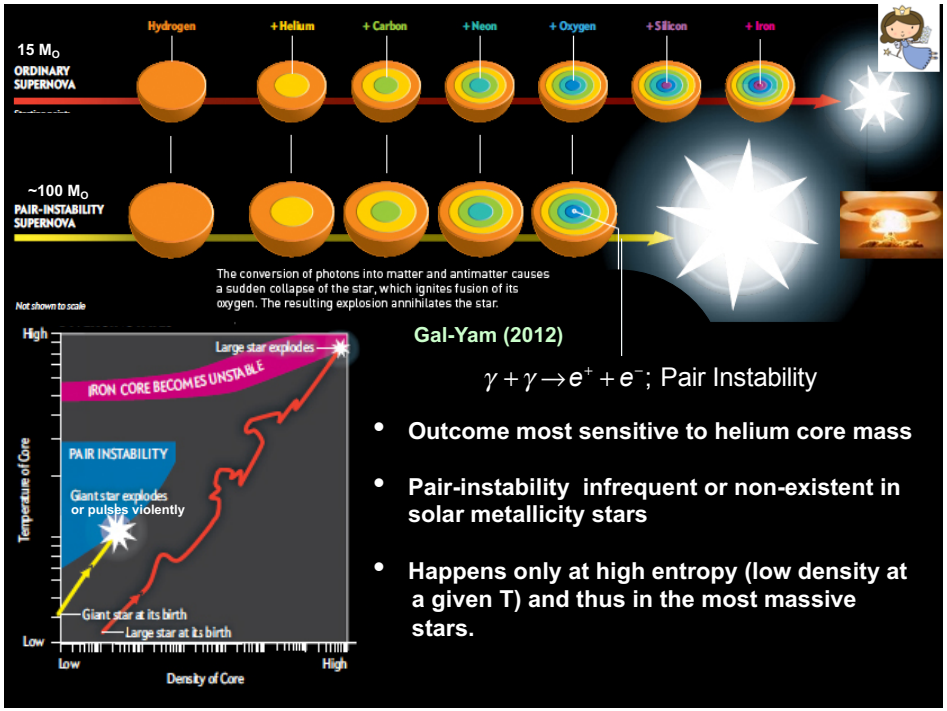

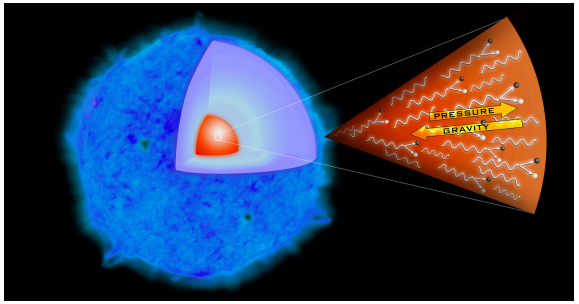

The bigger the star the greater the binding energy that must be provided to reverse the implosion. Thus bigger stars achieve a higher "bounce" temperature and burn more fuel to heavier elements.

There thus ends up being three regimes for pair instability:

1) The first explosion is unable to disrupt the star, so it contracts and tries again. Eventually fuel is exhaused and the remaining core collapses probably to a black hole (PPISN)

2) A single explosion disrupts the whole star (PISN)

3) Insufficient burning occurs to reverse the explosion on the first try and the star collapses to a black hole.

PAIR INSTABILITY SUPERNOVAE

He Core	Main Seq. Mass	Supernova Mechanism
$2 \le M \le 35$	$10 \le M \le 80$	Fe core collapse to neutron star or a black hole
$35 \le M \le 65$	$80 \le M \le 140$	Pulsational pair instability followed by Fe core collapse
$65 \le M \le 133$	$140 \le M \le 260$	Pair instability supernova (single pulse)
$M \ge 133$	$M \ge 260$	Black hole

e.g. Woosley, Blinnikov and Heger (Nature 2007)

Mass	T_c (K)	ρ_c (g cm^{-3})
65	1.741×10^9	3.158×10^5
70	3.570×10^9	2.001×10^6
75	3.867×10^9	2.544×10^6
80	3.876×10^9	2.316×10^6
85	4.025×10^9	2.479×10^6
90	4.197×10^9	2.699×10^6
95	4.355×10^9	2.902×10^6
100.....	4.533×10^9	3.195×10^6
105.....	4.720×10^9	3.577×10^6
110.....	4.931×10^9	4.079×10^6
115.....	5.140×10^9	4.637×10^6
120.....	5.390×10^9	5.423×10^6
125.....	5.734×10^9	6.766×10^6
130.....	6.169×10^9	9.012×10^6

Above 133 M_O collapse to a black hole

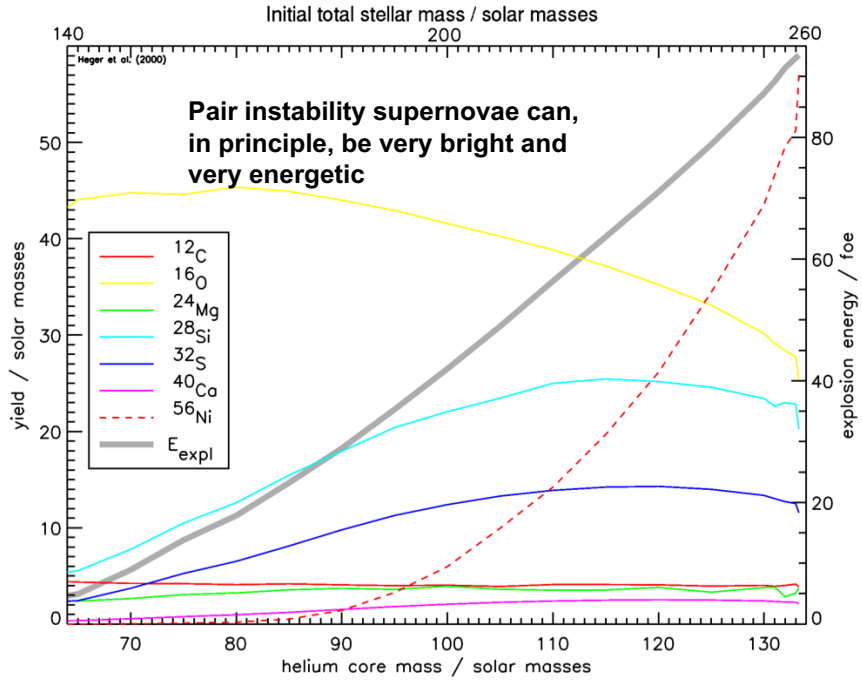

A wide variety of outcomes is possible

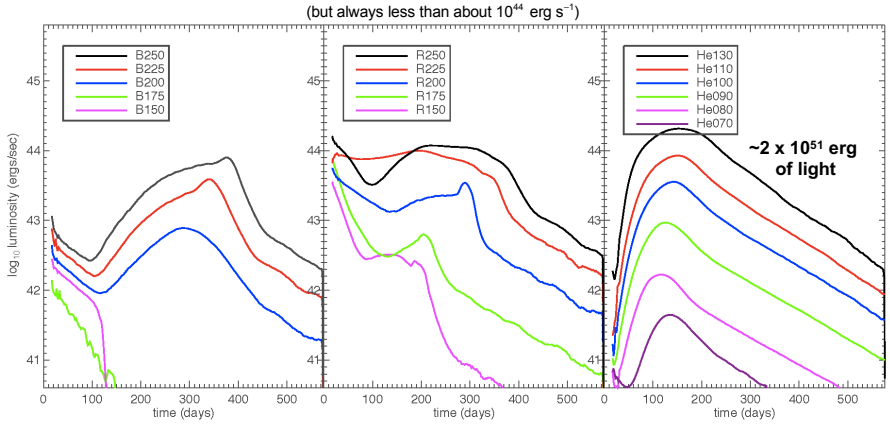

Blue Supergiants | Red Supergiants | Helium Cores

The light curve is a combination of envelope recombination (RSG and BSG) and radioactivity (He cores)

(e.g., Scannapieco et al 2005; Kasen, Woosley and Heger 2011; Kozyreva et al 2014; Kozyreva and Blinnikov 2015, etc.)

Red-shifted light curve of a bright pair-instability SN

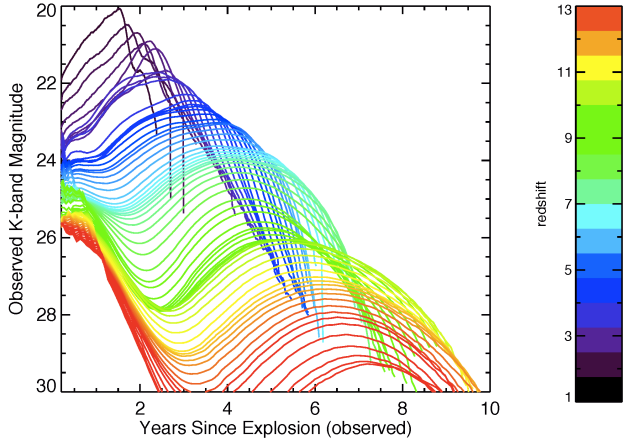

Fig. 12.— Observed K-band light curve of model R250 as a function of redshift. The effects of cosmological redshift, dimming, and time-dilation have all been included. For $z > 7$, one is observes the rest-frame UV, and the initial thermal component of the light curve is brighter than the later radioactively powered peak.

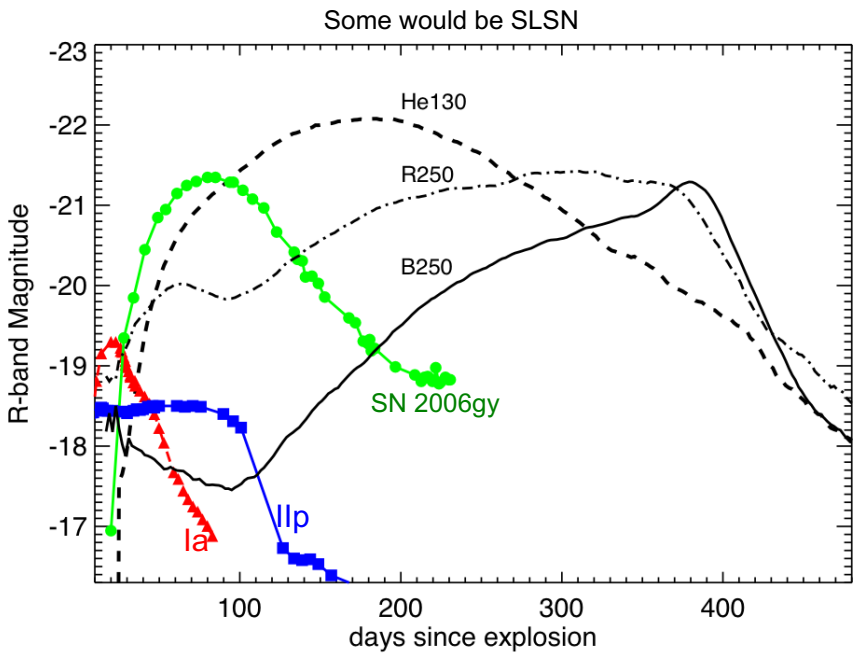
Some would be SLSN
R-band Magnitude
days since explosion
He130
R250
B250
SN 2006gy
Ia
IIp

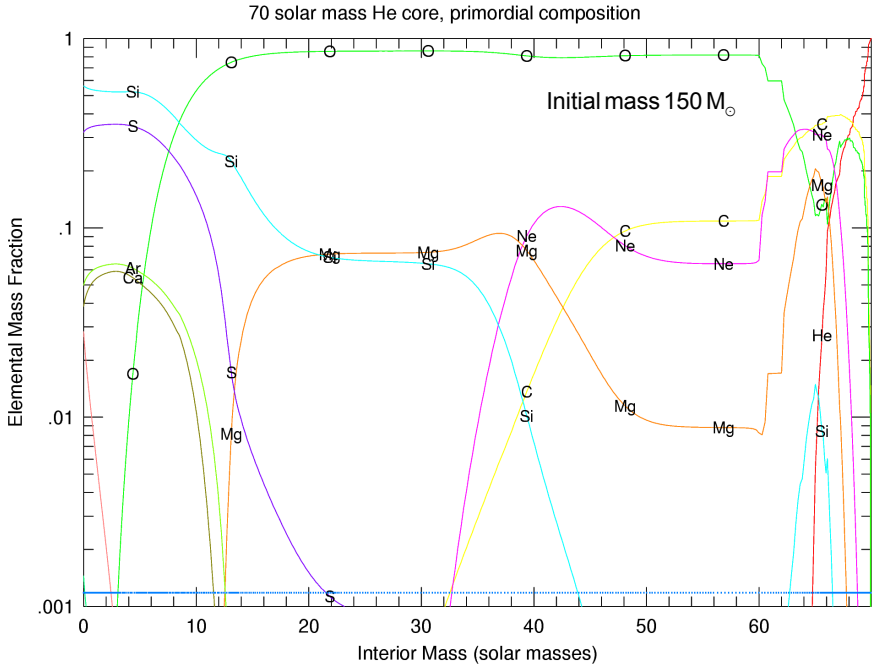
70 solar mass He core, primordial composition
Initial mass 150 M⊙
Elemental Mass Fraction
Interior Mass (solar masses)

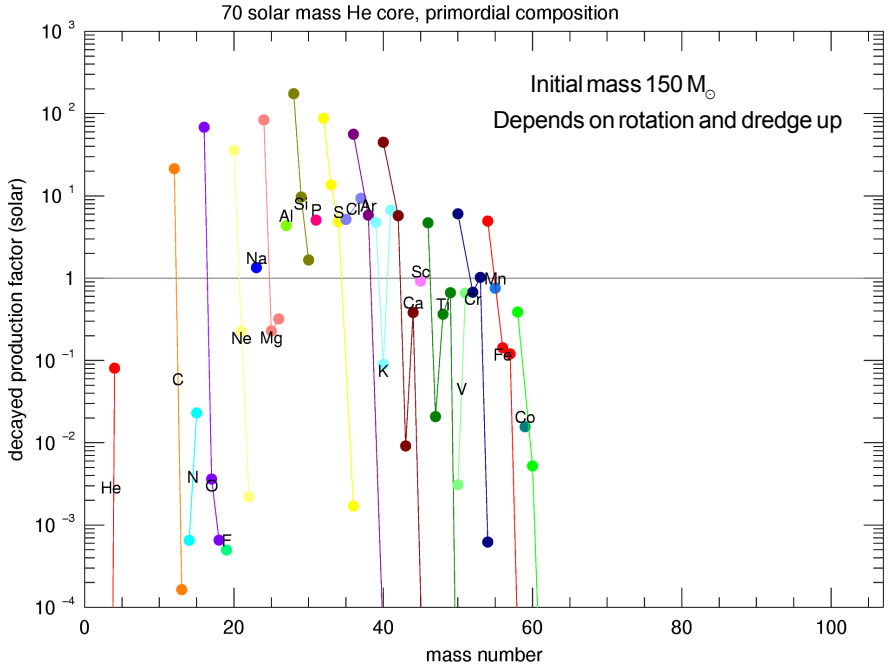
70 solar mass He core, primordial composition
Initial mass 150 M⊙
Depends on rotation and dredge up
decayed production factor (solar)
mass number

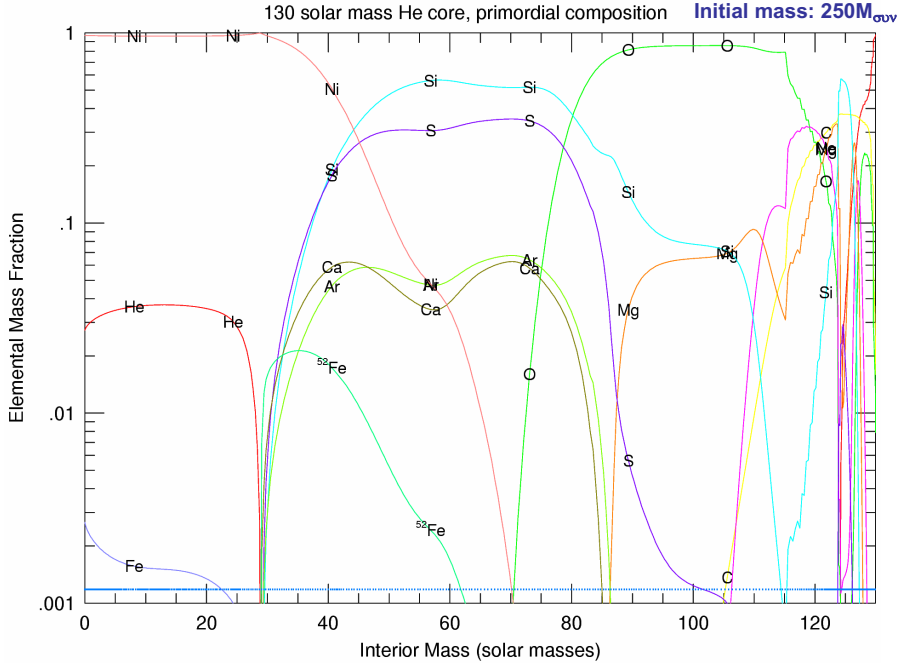
130 solar mass He core, primordial composition
Initial mass: 250M⊙
Elemental Mass Fraction
Interior Mass (solar masses)

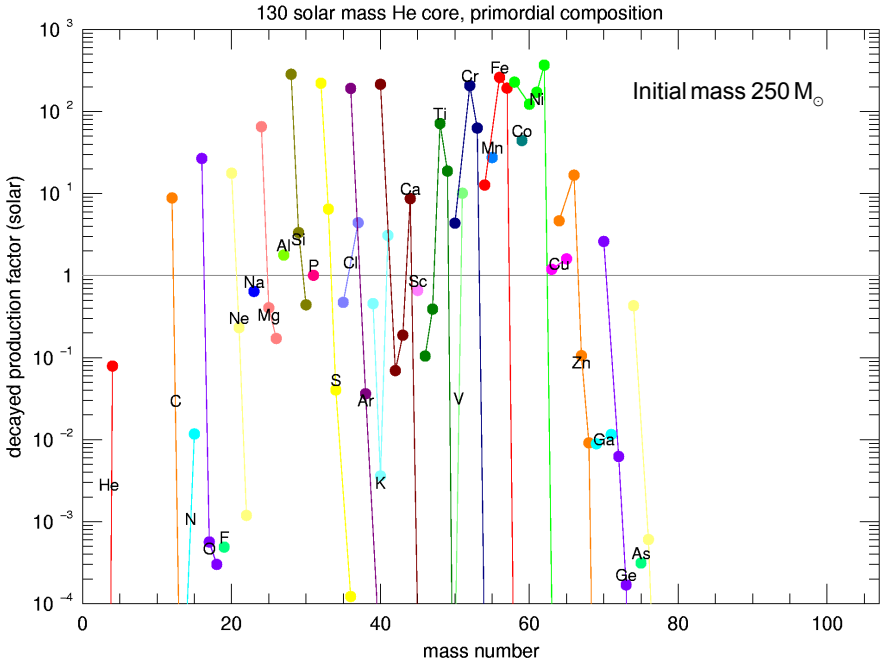

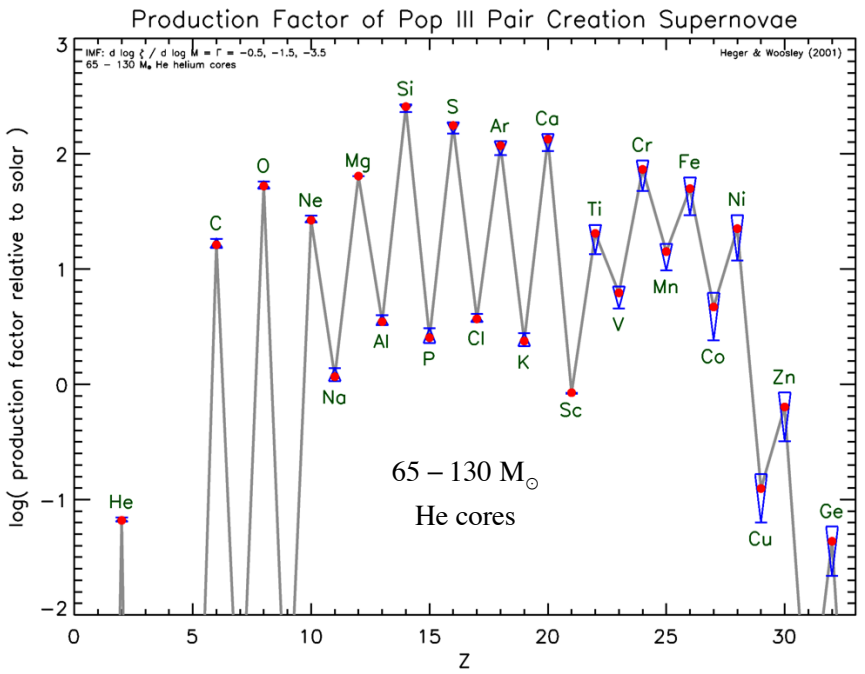

Big odd-even effect and deficiency of neutron rich isotopes.

Star explodes right after helium burning so neutron excess is determined by initial metallicity which is very small.

$$\mathrm{CNO} \rightarrow {}^{14}\mathrm{N}\,(\alpha,\gamma)\,{}^{18}\mathrm{F}\,(\mathrm{e}^{+}\upsilon)\,{}^{18}\mathrm{O}\,(\alpha,\gamma)^{22}\,\mathrm{Ne}$$

$$\eta \approx 0.002\left(\frac{Z}{Z_{\odot}}\right)$$

DO THEY HAPPEN?

- Major uncertainty – mass loss as a function of Z
- SN 2007bi (GalYam et al (2009) M_{He}~105$M_{\odot}$; 3 - 10 $M_{\odot}$ ^{56}Ni

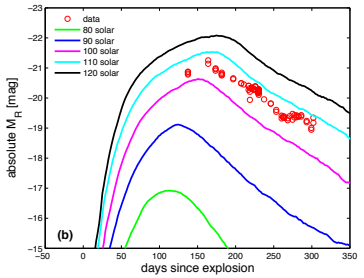

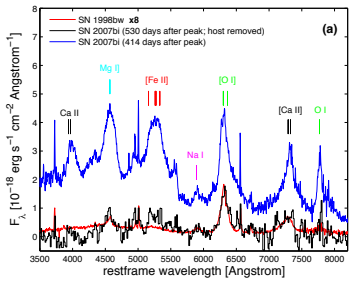

$Z_{host} \approx 1/3\ Z_{\odot}$

requires substantial reduction in standard mass loss

- Implies the existence of a much larger number of lighter pair and *pulsational pair SN* of lower mass.

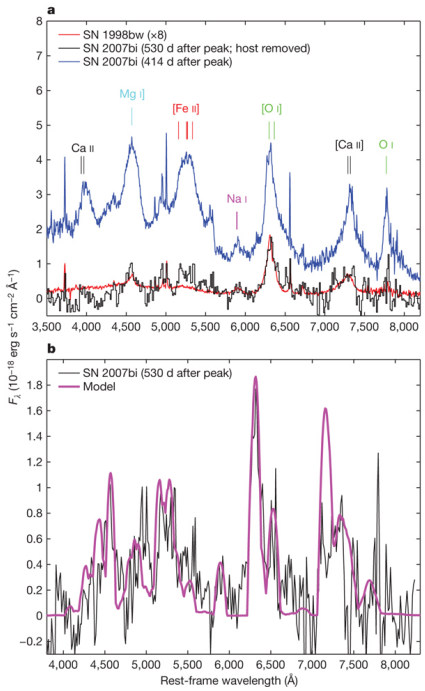

The late time spectrum suggests the presence of a lot of ^{56}Ni was made in the explosion (^{56}Fe by the time the observations were made).

But Mazzali et al (2019) say iron lines are too broad to be the result of a pair-instability model (too much mass)

Pulsational Pair Instability (should be more common than PSN)

Starting at helium core masses ~35 solar masses, or about 80 solar masses on the main sequence, post carbon-burning stars experience a pulsational instability in nuclear energy generation that comes about because of pair production

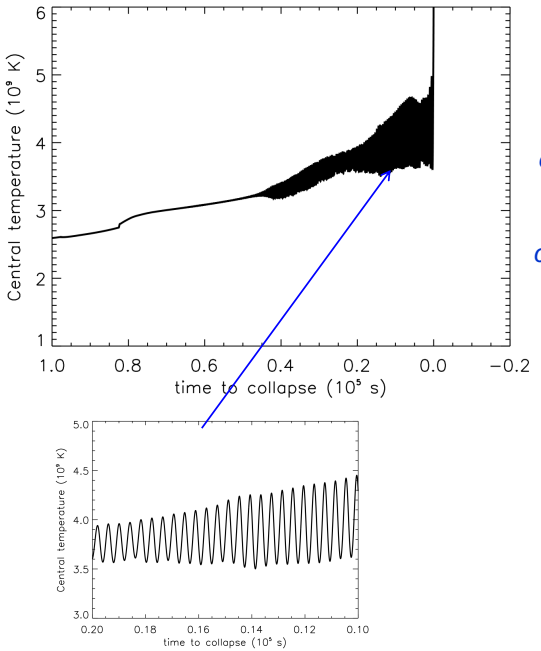

80 Solar masses
He core 35.7

*Pulsational instability begins shortly after central oxygen depletion when the star has about one day left to live (t = 0 here is iron core collapse). The unstable region is the oxygen **shell***

Pulses occur on a hydrodynamic time scale for the helium and heavy element core (~500 s).

For this mass, there are no especially violent single pulses before the star collapses..

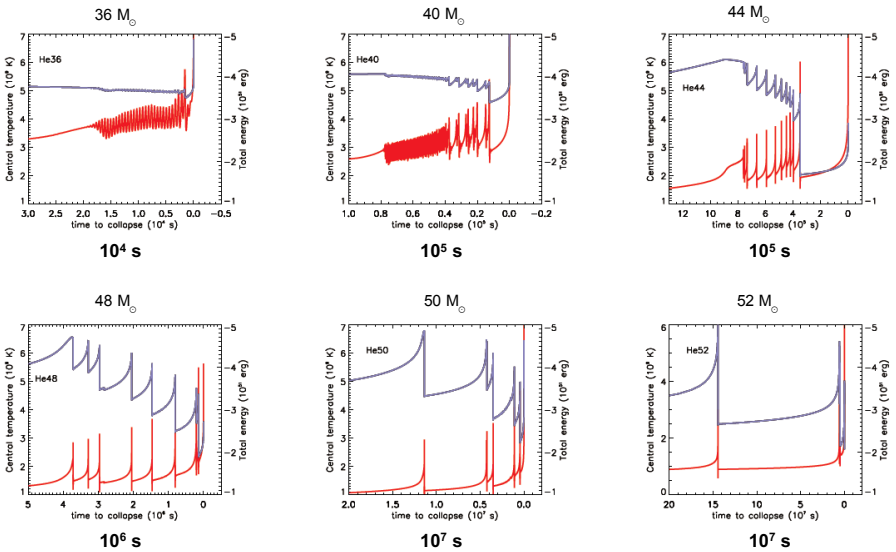

Central temperature and gravitational binding energy as a function of time (measured prior to iron core collapse for helium cores of 36, 40, 44, 48, 50 and 52 solar masses. As the helium core mass increases the pulses become fewer in number, less frequent, and more energetic

THE PULSATIONAL- PAIR ENGINE

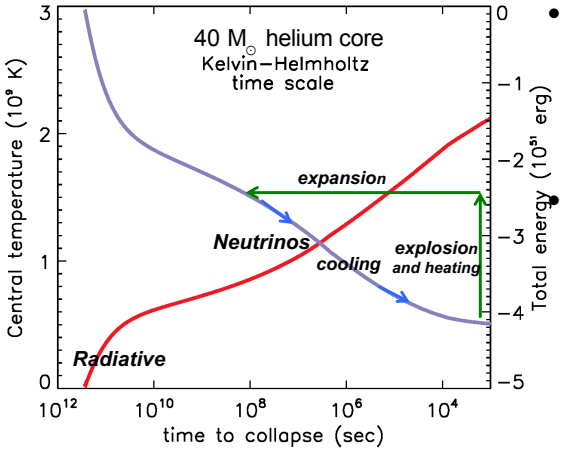

40 $M_\odot$ Kelvin-Helmholtz Contraction (no burning)

- More energetic pulses take a longer time to recur – more energy means expansion to a less tightly bound star
- Since 40 M_O is a typical core mass for PPISN, the maximum duration of all pulsing activity is about 10,000 yr. This is an upper bound to the pulsing activity There will be no PPISN that last longer. Models confirm this
- An explosion energy of ~4 x 10^{51} erg will unbind the star and make a PISN.

Over time this pulsing activity reduces the entropy and exhausts all fuel in the unstable region.

E.g., 50 $M_\odot$ helium core pulses until 46.7 $M_\odot$ is left then evolves to core collapse

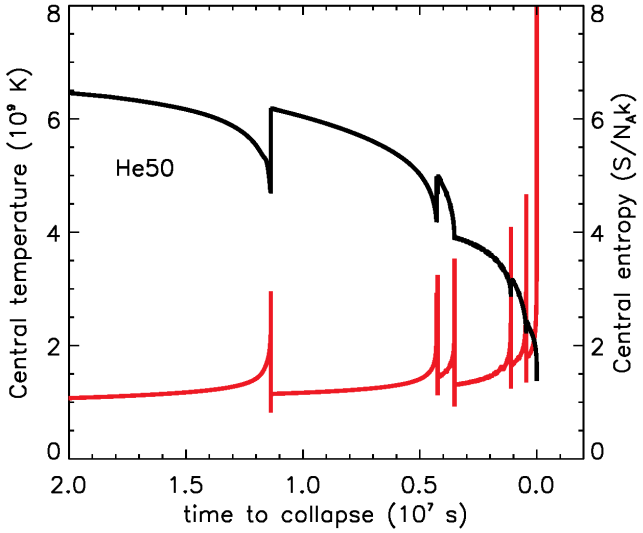

Pulsational Pair SN – Helium cores, no mass loss

Mass ($M_\odot$)	M_{CO} ($M_\odot$)	Pulses	Duration (sec)	KE-pulse (10^{51} erg)	M_{Fe} ($M_\odot$)	M_{eject} ($M_\odot$)	$M_{remnant}$ ($M_\odot$)
30	24.65	stable	-	-	2.34	-	30.00
32	26.30	stable	-	-	2.38	-	32.00
34	28.01	5 weak	2.3(3)	0.0012	2.51	0.13	33.87
36	29.73	33 weak	1.8(4)	0.0037	2.53	0.18	35.82
38	31.40	>100 weak	4.2(4)	0.0095	2.65	0.34	37.66
40	33.05	9 strong	7.8(4)	0.066	2.92	0.97	39.03
42	34.77	18	2.0(5)	0.26	2.68	2.65	39.35
44	36.62	11	7.7(5)	0.83	3.18	5.02	38.98
46	38.28	11	1.2(6)	0.77	2.40	5.51	40.49
48	40.16	8	3.8(6)	0.94	2.53	6.65	41.35
50	41.83	6	1.2(7)	0.86	2.76	6.31	43.69
51	42.59	6	1.9(7)	1.00	2.37	7.80	43.20
52	43.52	5	1.4(8)	0.99	2.47	7.87	44.13
53	44.34	4	7.8(8)	0.86	2.68	4.73	46.70
54	45.41	4	4.7(9)	0.94	2.16	6.85	47.15
56	47.14	3	3.4(10)	0.56	2.04	7.99	48.01
58	48.71	3	8.0(10)	1.1	2.00	12.14	45.86
60	50.54	3	8.5(10)	0.75	1.85	12.02	47.98
62	52.45	7	2.2(11)	2.3	3.19	27.82	34.18
64	54.14	1	-	4.0	-	64	-

Iron Core Probably Collapses to a Black Hole

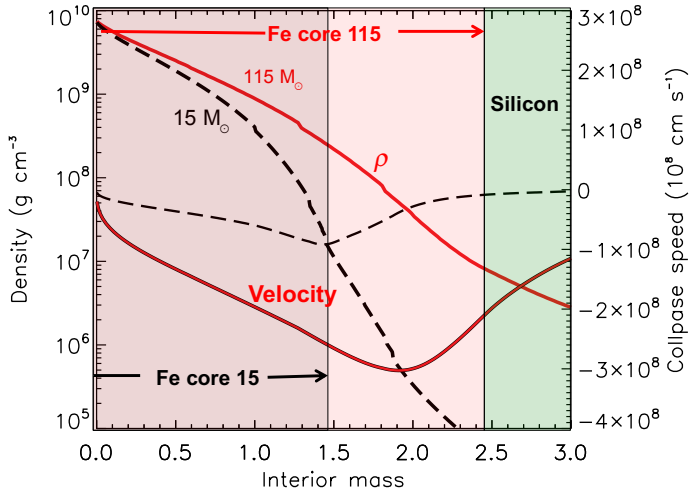

But the rotation rate can be substantial - milliseconds

Chritian Ott (private communication 2011)

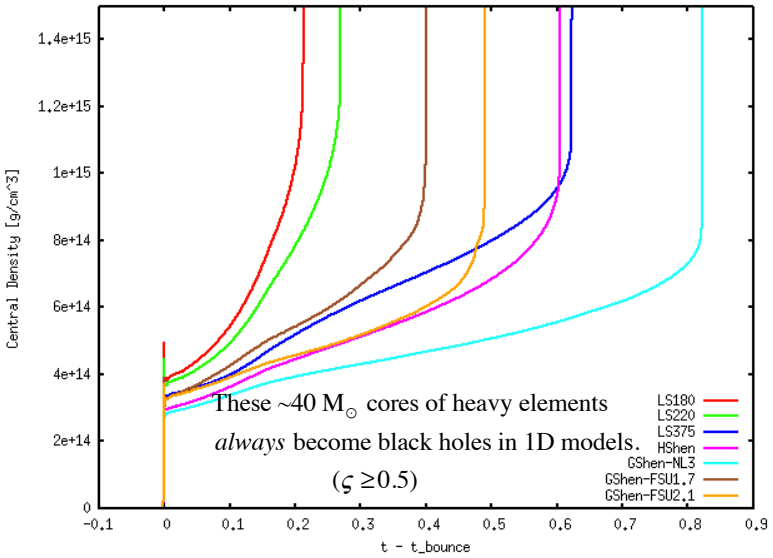

TOTAL ENERGY IN PULSES

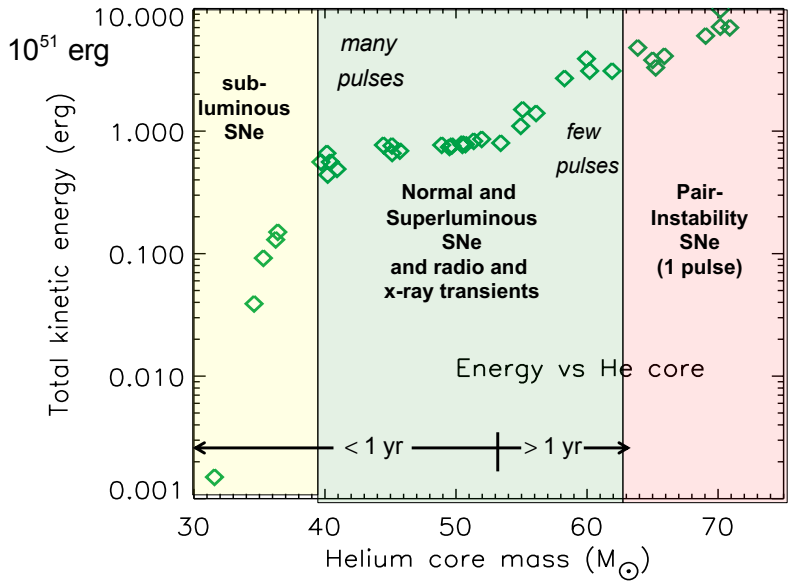

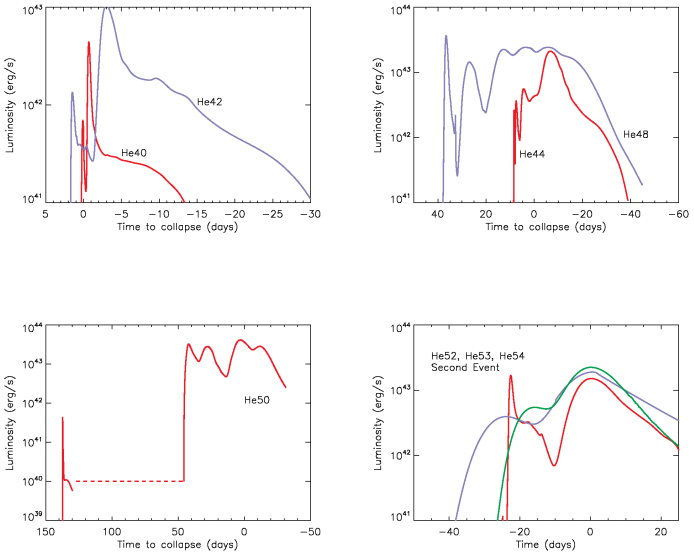

Hot (T = 10 – 20,000 K) low v (~3000 km s^{-1}) events

4.6, 24,5, and 149 years l after first event

Type II PPISN

TABLE 2. LOW METALLICITY MODELS

Mass ($M_\odot$)	Mass Loss	M_{preSN} ($M_\odot$)	M_{He} ($M_\odot$)	M_{CO} ($M_\odot$)	M_{Si} ($M_\odot$)	M_{Fe} ($M_\odot$)	Duration (10^7 sec)	M_{final} ($M_\odot$)	KE_{eject} (10^{50} erg)
T70	1	47.31	29.42	25.62	7.58	2.54	0.00066	47	-
T70A	1/2	51.85	30.10	26.41	7.87	2.58	0.00065	52	-
T70B	1/4	59.62	30.50	26.84	8.28	2.57	0.00072	60	-
T70C	1/8	64.66	30.72	27.14	8.22	2.54	0.00068	65	0.0005
T70D	0.	70	31.57	28.00	8.41	2.57	0.0012	52	0.015
T75	1	48.46	32.47	28.36	7.41	2.54	0.00075	41	0.0028
T75A	1/2	54.24	31.90	27.97	8.64	2.52	0.0014	42	0.024
T75B	1/4	62.97	33.07	29.15	8.71	2.64	0.0015	51	0.021
T75C	1/8	68.61	33.41	29.67	8.91	2.61	0.0016	51	0.029
T75D	0.	75	33.82	30.20	8.71	2.67	0.0019	50	0.11
T80	1	50.79	34.70	30.81	7.90	2.65	0.0019	39.6	0.19
T80A	1/2	55.32	34.59	30.74	8.38	2.62	0.0061	39.2	0.39
T80B	1/4	66.04	35.30	31.37	8.44	3.00	0.0098	34.7	0.92
T80C	1/8	72.76	36.24	32.28	8.03	3.29	0.014	34.8	1.3
T80D	0	80	36.40	32.56	7.93	3.09	0.015	34.9	1.5
T90	1	55.32	38.77	34.58	7.16	2.73	0.039	37.3	2.6
T90A	1/2	60.62	39.69	35.37	9.54	2.57	0.11	35.9	4.1
T90B	1/4	72.16	40.41	36.16	9.54	2.84	0.18	36.4	5.2
T90C	1/8	80.61	40.21	36.00	6.22	2.87	0.20	37.4	4.9
T90D	0	90	40.92	36.78	8.35	2.86	0.19	37.1	4.9
T100	1	57.58	44.85	39.65	4.56	2.48	1.0	38.9	7.0
T100A	1/2	62.20	44.46	39.74	5.24	2.73	0.74	39.3	7.7
T100B	1/4	78.58	45.11	40.61	4.64	2.44	0.92	39.9	7.6
T100C	1/8	88.11	45.71	41.23	4.67	2.53	1.7	40.4	6.9
T100D	0	100	45.13	40.70	6.44	2.87	0.45	40.4	6.6
T105	1	59.54	47.52	42.00	4.78	2.79	7.34	43.6	7.8
T105A	1/2	66.88	46.04	41.45	4.78	2.62	1.22	40.8	8.0
T105B	1/4	81.18	47.34	42.55	5.75	2.92	2.20	42.5	7.8
T105C	1/8	91.94	48.33	43.56	4.70	2.73	4.38	44.2	7.0
T105D	0	105	49.45	44.67	4.87	1.97	10.7	44.8	7.8
T110	1	63.31	49.89	44.39	4.92	1.98	17	45.1	8.6
T110A	1/2	68.41	49.68	44.58	4.88	1.95	39	44.5	7.6
T110B	1/4	84.13	49.50	44.67	4.70	2.18	9.5	44.7	7.4
T110C	1/8	95.98	48.91	44.19	4.53	2.59	5.8	44.8	7.1
T110D	0	110	50.49	45.44	4.75	2.08	30	45.0	7.7

T120A	1/2	79.55	55.08	49.16	4.60	2.60	460	50.6	15
T120B	1/4	90.11	53.41	48.21	4.65	2.52	250	48.2	8.0
T120C	1/8	103.3	54.94	49.79	4.31	2.03	350	51.8	11
T120D	0	120	56.11	50.52	4.75	2.18	1200	51.8	14
T121A	1/2	73.09	54.67	49.14	4.74	2.03	460	50.9	11
T122A	1/2	73.94	56.06	49.76	6.05	2.24	12000	44.9	31
T123A	1/2	74.38	55.79	50.38	5.36	1.74	3900	50.2	17
T124A	1/2	74.39	56.85	50.58	6.24	2.30	12000	46.9	35
T125	1	69.21	57.49	51.75	5.49	1.78	6500	50.3	13
T125A	1/2	81.38	57.12	51.20	5.79	1.90	8600	51.8	16
T125B	1/4	92.24	57.08	51.53	5.44	1.70	4900	50.9	15
T125C	1/8	107.1	57.58	52.08	5.69	2.43	11000	49.0	14
T125D	0	125	56.20	51.75	4.89	2.58	7400	47.8	11
T130	1	71.00	60.50	54.62	6.75	2.41	15000	50.8	23
T130A	1/2	79.69	60.20	54.28	6.03	1.81	10000	51.3	33
T130B	1/4	94.26	58.28	53.48	8.16	3.75	13000	48.4	27
T130C	1/8	110.6	61.91	56.10	8.99	3.95	16000	49.0	31
T130D	0	130	59.96	54.28	2.04	2.04	25000	38.8	41
T135	1	71.37	64.04	56.60	5.43	3.83	140	18.9	42
T135A	1/2	85.71	65.42	56.36	5.56	3.27	19000	43.3	38
T135B	1/4	97.54	61.15	55.30	5.39	3.05	18000	42.9	35
T135C	1/8	107.2	60.14	54.71	2.41	2.07	4500	23.2	31
T135D	0	135	63.91	57.54	4.37	2.84	4300	35.0	39
T140	1	75.29	65.63	58.32	5.48	-	-	0	44
T140A	1/2	89.64	65.90	59.55	5.54	1.95	200	4.5	41
T140B	1/4	99.08	65.01	59.06	4.25	2.65	110	29.2	38
T140C	1/8	108.6	63.87	57.96	6.04	-	-	0	48
T140D	0	140	65.24	59.19	5.20	2.63	21000	37.4	33
T150	1	76.38	71.63	64.73	6.83	-	-	0	120
T150A	1/2	95.98	70.89	64.20	5.99	-	-	0	70
T150B	1/4	106.4	69.05	62.76	6.11	-	-	0	60
T150C	1/8	113.4	70.17	63.94	5.93	-	-	0	71
T150D	0	150	70.18	64.86	6.41	-	-	0	98

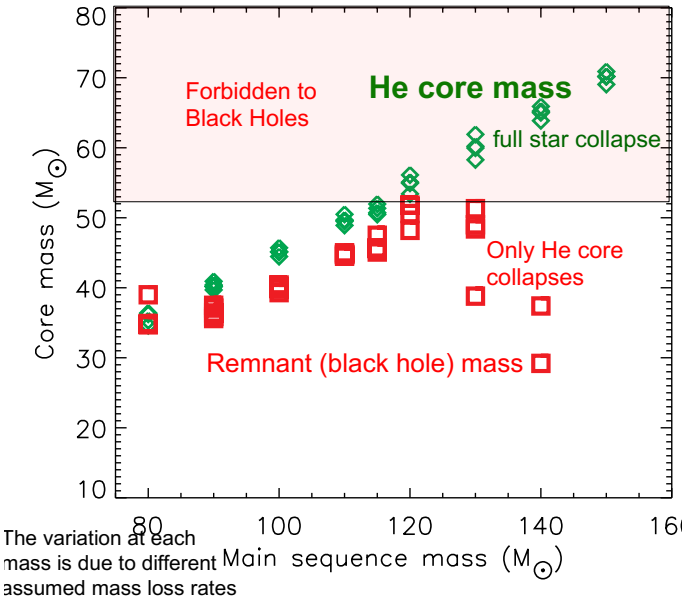

No black holes will be born with mass between 52 and 133 solar masses if they are in close binaries. Many will have masses near 35 – 50 solar masses

No remnant until 260 M_O

The variation at each mass is due to different assumed mass loss rates in the precollapse star

EXPLOSIONS IN RED SUPERGIANTS (10% Z_O)

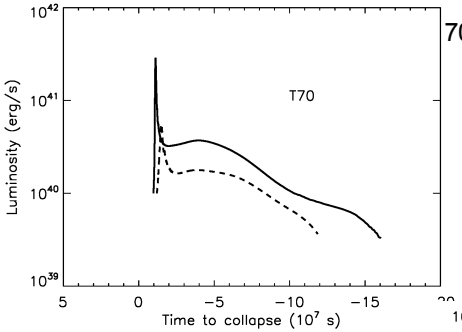

70 $M_\odot$ - barely unbind part of the hydrogen envelope. Faint red (3000 K) slow transients - several years. Luminosity less than 10^{41} erg s^{-1}, speeds ~ 100 km s^{-1}. Mass of envelope depends on mass loss history.

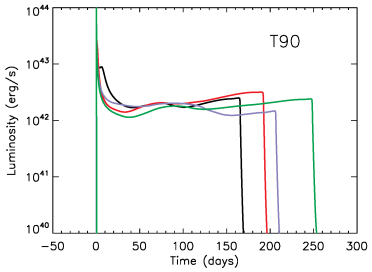

90 $M_\odot$ - rather ordinary SN IIp but no radioactive tails

80 $M_\odot$ - entire envelope ejected. Duration of pulses much less than duration of plateau. Total energy less than 10^{51} erg. Faint to normal SN IIp. Peak L ~ 10^{42} erg s^{-1}

THESE MAY BE COMMON EVENTS

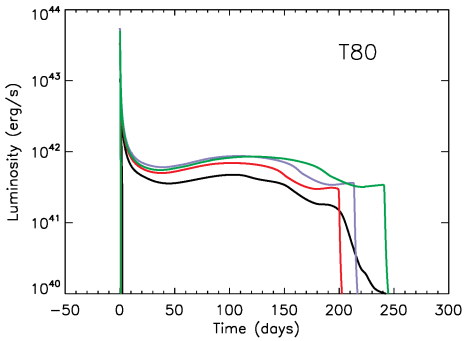

100 $M_\odot$ – structured light curves with the effects of multiple pulses becoming visible. Shells colliding while SNis in progress.

L_{max} ≈ 0.5 - 1 x 10^{43} erg s^{-1}

Total light 1 - 2 x 10^{50} erg

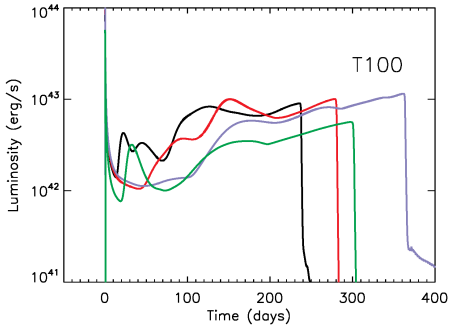

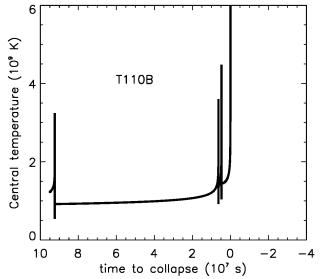

Now it gets interesting. The helium core has reached 50 solar masses and strong pulses are occurring over a period of years rather than months

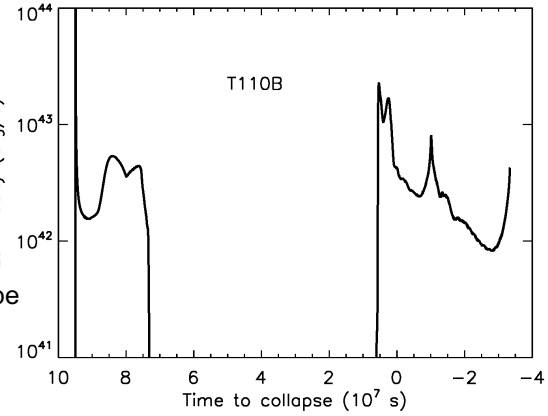

The first pulse ejects the entire envelope in a rather ordinary SN Iip. That will be the case for heavier stars as well. Subsequent pulses eject He and CO rich shells that run into the H-He envelope and make bright long-lasting structured events

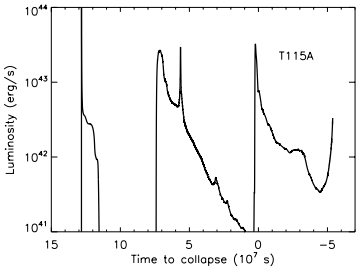

Moving up in mass the intervals between pulses becomes longer and the pulses more energetic. Supernovae can be separated by long intervals during which the star remains shining with a luminosity near 10^{40} erg s^{-1}

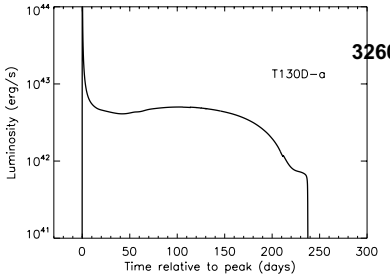

3260 years later …

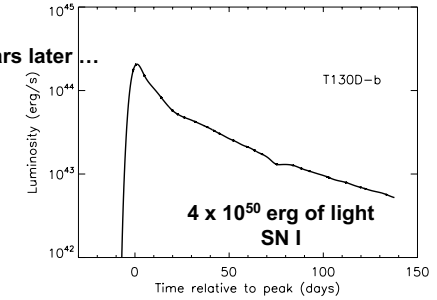

PPISN SLSN TYPE II SUMMARY – NO ROTATION

- Faint long red transients common, 10^{40} – 10^{42} erg s^{-1}
- Luminosities of 10^{43} – 10^{44} erg s^{-1} possible for up to ~400 days. He cores that make bright optical transients are in a narrow mass range 48 – 55 solar masses and hence relatively rare.
- Total energy in both light and ejected mass cannot exceed 4 x 10^{51} erg (from pulses alone)
- Can be preceded by an “ordinary” SN IIp a few years earlier
- Light curves can be highly structured with several major peaks
- More energetic longer events may make radio and X-ray SNe lasting centuries
- Leave a population of 35 – 52 solar mass black holes

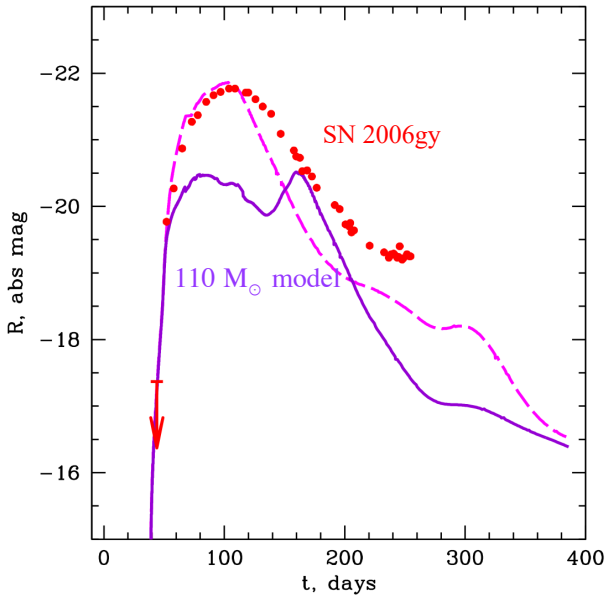

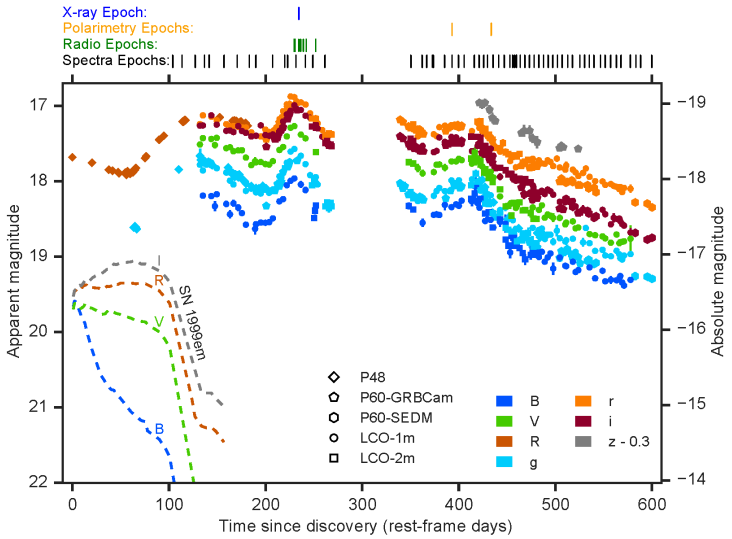

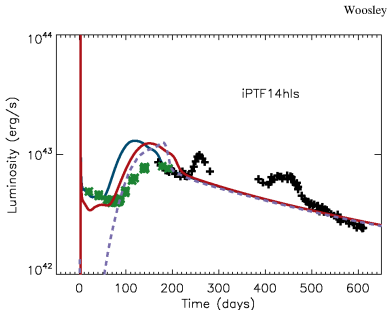

20 M_O red supergiant 1 B explosion +
Magnetar B = 4 x 10^{13} G, initial period 6 ms (6 x 10^{50} erg)
See also Dessart (2017)

Right: PPISN model based on a 115 M_O star. Two explosions. Top panel is first explosion. Bottom panel is second explosion 46 years later.

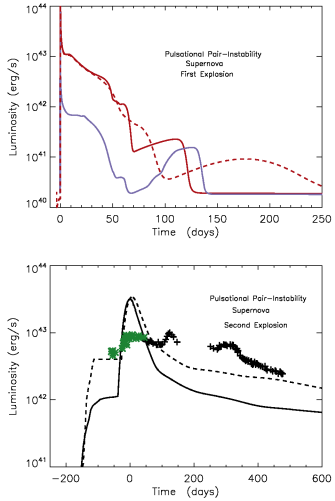

Figure 5. Light curves from pulsational events in Model T115. (Top:) Light curve from the first pulse which ejects of most of the hydrogen envelope. The solid red line is for the standard red supergiant progenitor and the blue line is for a blue supergiant progenitor. The dashed red line shows the effect of using a larger floor to the opacity. After about 80 days most of the luminosity is due to fallback and accretion and is quite uncertain. (Bottom:) 46 years later, two pulses separated by 130 days eject shells that collide with themselves and with the previously ejected envelope producing the light curve shown. The solid curve is the standard model. The dashed curve results if the velocity of the leading edge of pulse 2 is increased by 50%. Green and black points are the observed light curve of iPTF14hls (Arcavi et al. 2017) (see text).

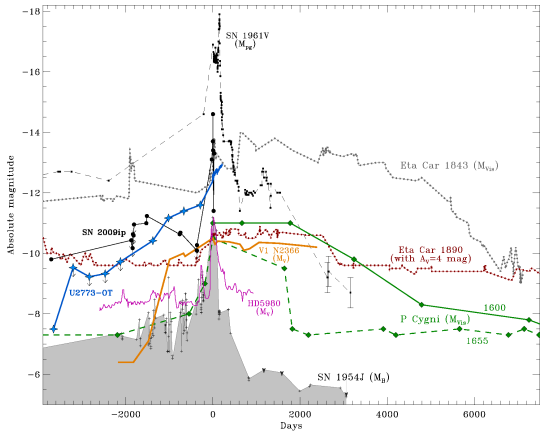

1961v - one of the strangest supernovae. Zwicky's original Type 5. Progenitor was visible for years as a very bright M ~ -12 star. Catgorized later as a supernova imposter, but bright as an ordinary supernova.

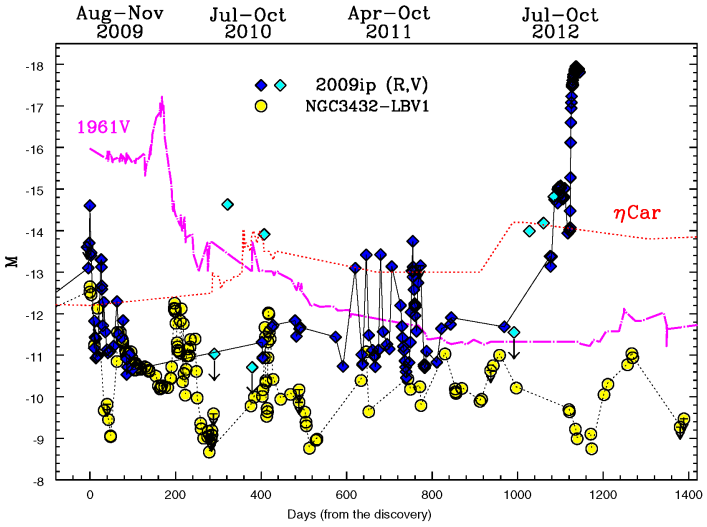

Figure 2. *R*-band absolute light curve of SN 2009ip (blue diamonds) compared with those of the impostor NGC 3432-LBV1 (yellow circles), the debated SN/impostor 1961V (photographic plate magnitudes, magenta dot-dashed line), and the historical visual light curve of η Carinae during the period 1842–1845 (revised by Smith & Frew 2011, red dotted line). The cyan diamonds represent CRTS *V*-band measurements (see also Drake et al. 2010, 2012). The data showing NGC 3432-LBV1 during the period 2008–2012 are from Pastorello et al. (2010), plus additional recent unpublished observations (see Table 4). The epoch 0 of the η Carinae light curve is year 1842.213 (UT). The erratic photometric variability is a common property of major eruptions of LBVs.

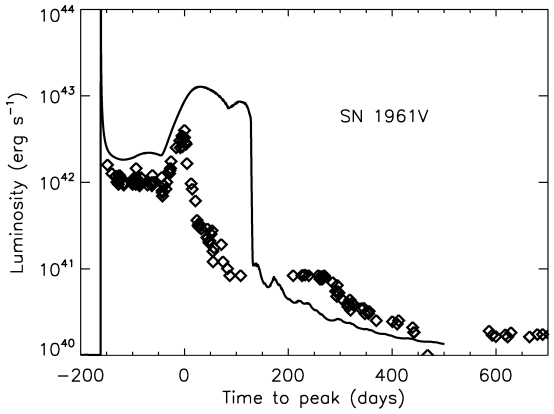

105 M_O pulsational pair instability. Fits preSN luminosity, duration, brightness, ~velocity. Hard to get short second peak.

Inserra

The Astrophysical Journal, 767:1 (19pp), 2013 April 10

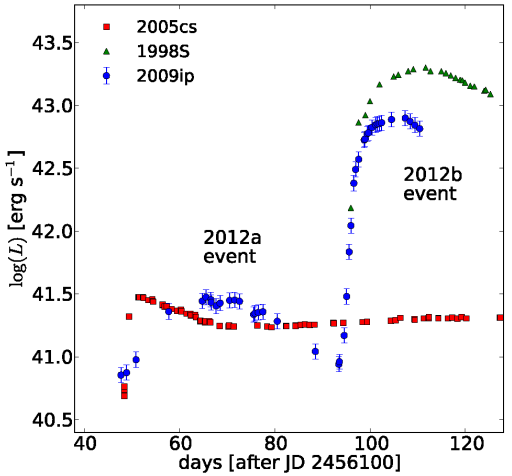

Figure 4. Bolometric light curve of SN 2009ip from 2012 August to October (showing both the 2012a and 2012b events), compared with the bolometric light curves of the faint type IIP SN 2005cs (Brown et al. 2007; Pastorello et al. 2006, 2009) and the type IIn/IIL SN 1998S (Liu et al. 2000; Fassia et al. 2000; Gerardy et al. 2002; Pozzo et al. 2004). The light curves of SNe 2005cs and 1998S are shown in an arbitrary temporal scale to match well, respectively, the 2012a and 2012b eruptive events of SN 2009ip.

PPSN – Nucleosynthetic Implications

Since anywhere from most to all of the carbon oxygen core collapses to a black hole the nucleosynthesis is limited to what exists in the hydrogen envelope (H, He, plus CNO from dredge up), and some elements from the outer helium core (C, O, Ne, Mg). In particular there is no explosive nucleosynthesis and no iron group elements are made.

This is especially interesting for first generation (Pop III) stars.

Qualitative agreement with what is seen in the oldest stars in the galaxy – the ultra-iron-poor stars

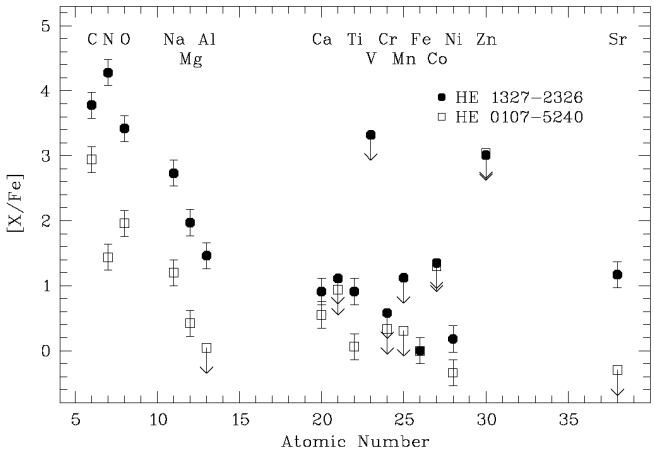

Frebel et al (2008)

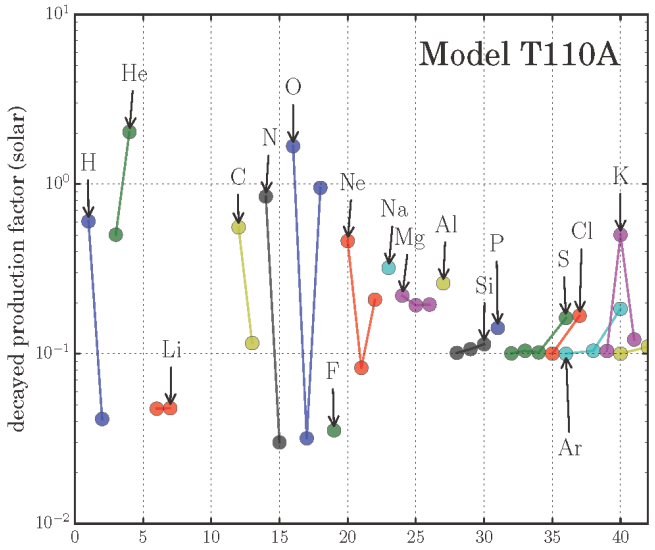

Anything near 0.1 was not made in the star. Nothing produced above Ca.

Paths to a Rapidly Rotating Core

- **Chemically homogeneous evolution** – the star is rapidly on the main sequence and mixes completely. At the end of core hydrogen burning, there is very little hydrogen left on the surface. Giant formation and the consequent braking of the core is avoided. If the metallicity is low, mass loss from the helium star is avoided and the core retains high angular momentum – Maeder (1987) Woosley and Heger (2006)

- **Merger in a massive binary** - If the initial masses of two stars are within 5 – 10% of one another, the merger may happen when both stars have already developed helium cores leading to a double core common envelope stage (Brown 1995, Dewi et al 2006). But would the envelope be fully ejected?

Paths to a Rapidly Rotating Core

- **Tidally locked WR -** Need a short orbital period which may mean the companion is a neutron star or black hole. Detmers et al (2008). Cygnus X-3 is a WR star with a compact companion.

- **Change the standard physics** – Weaker magnetic torques than described by Spruit. Less mass loss as a WR star. Low metallicity.

SYNTHESIS - SLSN

- As of 2019, it seems like magnetars are the probable explanation for the majority of SLSN-I activity but with PPISN and CSM interaction playing important roles especially for SNSN-II

- No unambiguous evidence yet for a pair-instability supernova. SN 2006bi is a possible exception but there are many caveats Ruling out PISN, there is no unambiguous case of radioactivity powering a SLSN, though it does play a role in making SN Ic-BL with GRBs

- Limiting energy from a magnetar is 2 x 10^{52} erg in most cases

- PPISN and PISN can make a very diverse range of phenomena from very faint to very bight supernovae, long and short supernovae, recurrent supernovae, and supernovae with precursors

- PPISN and PISN are very rare though because of mass loss. Rapid rotation and binary mergers might bring the threshold down a bit

- At least one GW source seems to have been a PPISN. Verifying the predicted mass gap (46 – 133 M_O) in the future will be strong evidence for PPISN

- An area of intense observational activity. Hard for theory to keep up.